Chemical Science

Accepted Manuscript

This article can be cited before page numbers have been issued, to do this please use: W. Zhou, Y. Chen, Q. Yu, P. Li, X. Chen and Y. Liu, *Chem. Sci.*, 2019, DOI: 10.1039/C9SC00026G.

ROYAL SOCIETY OF CHEMISTRY

rsc.li/chemical-science

ROYAL SOCIETY OF CHEMISTRY
View Article Online
DOI: 10.1039/C9SC00026G

Journal Name

ARTICLE

Received 00th January 20xx,
Accepted 00th January 20xx

DOI: 10.1039/x0xx00000x

www.rsc.org/

Photo-responsive Cyclodextrin/Anthracene/Eu^{3+} Supramolecular Assembly for a Tunable Photochromic Multicolor Cell Label and Fluorescent Ink

Weilei Zhou,[a] Yong Chen,[a] Qilin Yu,[a,c] Peiyu Li,[a] Xuman Chen[a] and Yu Liu*[a,b]

A photo-responsive supramolecular assembly was successfully constructed through the stoichiometric 2:1 non-covalent association of two 4-(anthracen-2-yl)pyridine-2,6-dicarboxylic acid (**1**) in one γ-cyclodextrin (γ-CD) cavity, followed by the subsequent coordination polymerization of γ-CD·$\mathbf{1}_2$ ($\mathbf{1}_2$ = two **1**) inclusion complex with Eu(III). Interestingly, owing to the photodimerization behavior of anthracene units and the excellent luminescence property of Eu(III), the Eu^{3+}⊂γ-CD·$\mathbf{1}_2$ system showed multicolor fluorescence emission from cyan to red by irradiating for 0 - 16 minutes. Moreover, white light emission with CIE coordinates (0.32, 0.36) was achieved at 4 min. Importantly, white light-containing multicolor emission could be obtained in water, solid film and living cells. Especially, the Eu^{3+}⊂γ-CD·$\mathbf{1}_2$ system could tag living cells with marvelous white fluorescence and display no obvious cytotoxicity. Thus, this supramolecular assembly offers a new pathway in the field of tunable photochromic fluorescence ink and cell labelling.

Introduction

Pseudorotaxanes and rotaxanes as one typical species of molecular machines are challenging and interesting due to their mechanically interlocked topologies[1] and unique photophysical properties, leading to the widely applications in biomedicine[2], nanotechnology[3], smart materials[4] and so on. In particular, functional fluorescent rotaxanes[5] are of major importance, which draw more and more attentions by scientists and engineers. Multicolor emission, especially white-light emission, have various applications in solid-state lighting[6] and display media owing to their superior color fidelity and low color distortion.[7] Generally, white light emission could be achieved by different methods in inorganic and organic materials.[7b,8] Among them, the mixing of several fluorophores with complementary emission colors become a popular strategy,[9] and the dynamic reversible property of supramolecular system and molecular assembly strategy played an important role. For instance, Tian et al.[10] reported a white-light emission supramolecular assembly by changing the excitation wavelength and host–guest interactions in water. Tao et al.[11] reported a white-light emission supramolecular polymer based on cucurbituril and oligo (p-phenylenevinylene) by altering different amounts of cucurbit[8]urils in supramolecular assembly. Recently, we constructed a host–guest complexes by dipolar dyes styrylpyridiniums and cucurbituril in which the white-light emission was obtained by the addition of cucurbit[7]urils to methylated styrylpyridiniums for adjusting the stacking direction in water.[12]

Materials in response to externally photo-modulating, accompanied with the changes in physicochemical properties have draw much attention to extensively research because of potential applications in the various fields. Among all kinds of the stimuli-responsive artificial devices, it is beneficial to design luminescent materials based on lanthanide ions due to their unique luminescence properties, such as long-lived excited states, visible-light emission and narrow emission bandwidths, which could be easy to distinguish from shorter-lived (ns-based) autofluorescence from biological material.[13] Although the multicolor luminescence has been reported several times recently, the studies on the in-situ technique are still rare,[7c] particularly photo-tuning single lanthanide ion for multicolor luminescence including white light in aqueous solution remains a challenge. Herein, combining photo-tunable luminescent lanthanide,[13c] photo-erasable fluorescent ink[14] and cell imaging[15] of our previous reports, we designed a light-sensitive rotaxane network in aqueous solution from γ-cyclodextrin (γ-CD), 4-(anthracen-2-yl)pyridine-2,6-dicarboxylic acid (**1**) and Eu(III) as showed in Fig. 1. The complexation of γ-CD with **1** in 1:2 molar ratio led to the formation of a pseudo[3]rotaxane in aqueous solution. Furthermore, Eu(III) could coordinate with the carboxylic groups of pseudo[3]rotaxanes resulting in the formation of supramolecular network assembly. Significantly, the multicolor fluorescence emission varying from cyan→white→red could

[a] College of Chemistry, State Key Laboratory of Elemento-Organic Chemistry, Nankai University.
[b] Collaborative Innovation Center of Chemical Science and Engineering, Tianjin 300072, P. R. China.
[c] Key Laboratory of Molecular Microbiology and Technology, College of Life Sciences, Nankai University.
Electronic Supplementary Information (ESI) available: See DOI: 10.1039/x0xx00000x

be achieved by irradiating the pseudorotaxane network for 0 - 16 minutes, and these white light-containing multicolor emission consequently enabled the potential applications of pseudorotaxane network as tunable photochromic fluorescence ink and cell labelling. This supramolecular approach to obtain multicolor and white light emission by controlling the photoirradiation time would provide a new strategy for smart optical materials.

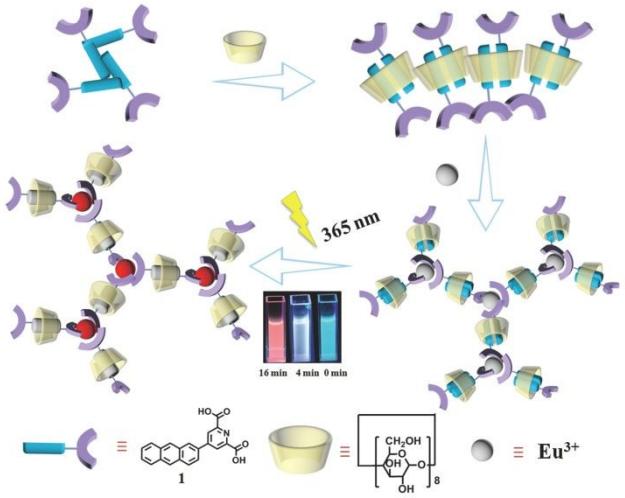

Fig. 1 Schematic illustration of γ-cyclodextrin/anthracene/Eu^{3+} supramolecular assembly and tunable lanthanide luminescence driven by reversible photo-cyclodimerization.

Experimental

Materials and methods

All chemicals were commercially available unless noted otherwise. Compound **4** was prepared according to the literatures procedure.[16] Compounds **2**, **5** and **6** were purchased from Heowns. NMR spectroscopy was recorded on a Brucker AV400 spectrometer. Fluorescence spectroscopy was recorded in a conventional quartz cell (light path 10 mm) on a Varian Cary Eclipse equipped with a Varian Cary single-cell peltier accessory to control temperature at 25 °C. UV/Vis spectra and the optical transmittance were recorded at 25 °C in a quartz cell (light path 10 mm) on a Shimadzu UV-3600 spectrophotometer equipped with a PTC-348WI temperature controller. High-resolution Transmission electron microscopy (TEM) images were acquired using a Tecnai 20 high-resolution transmission electron microscope operating at an accelerating voltage of 200 keV. The sample for high-resolution TEM measurements was prepared by dropping the solution onto a copper grid. The grid was then air-dried. Scanning electron microscopy (SEM) images were obtained using a Hitachi S-3500N scanning electron microscope. Dynamic Light Scattering (DLS) spectroscopy was examined on a laser light scattering spectrometer (BI-200SM) equipped with a digital correlator (TurboCorr) at 636 nm at a scattering angle of 90°. The hydrodynamic diameter (Dh) was determined by DLS experiments at 25°C. Electrospray ionization mass spectra (ESI-MS) were measured by Agilent 6520 Q-TOF-MS. Quantum yields were measured by an Edinburgh Instruments FS5 near-infrared spectrometer, with a 450 W xenon lamp as the excitation source. The 0.1 mM Eu^{3+}⊂γ-CD·$\mathbf{1}_2$ (pH=9) solution were used to measure the quantum yield of irradiation for 0 min with an excitation of 365 nm, and the collection range was from 345 nm to 800 nm. The quantum yield of Eu^{3+}⊂γ-CD·$\mathbf{1}_2$ solution after irradiation for 4 min and 16 min were respectively measured with an excitation of 290 nm, and the collection range was from 260 nm to 800 nm. Human lung adenocarcinoma cells (A549 cells, purchased from the Cell Resource Center, China Academy of Medical Science, Beijing, China) were cultured in F12 medium containing 10 % fetal bovine serum (FBS). A549 cells were seeded in 96-well plates (5×10^4 cell mL^{-1}, 0.1 mL per well) for 24 h at 37 °C in 5 % CO_2, and then incubated with Eu^{3+}⊂γ-CD·$\mathbf{1}_2$ ([Eu^{3+}]= 2 μM, [γ-CD] = 4 μM, [$\mathbf{1}_2$] = 8 μM) for another 24 h. The relative cellular viability was determined by MTT assay. A549 cells were seeded in 6-well plates (5×10^4 cell mL^{-1}, 2 mL per well) for 24 h at 37 °C in 5% CO_2. The cells were incubated with the corresponding solution for 12 h. After removing the medium, the cells were washed with phosphate buffer solution for three times and fixed with 4 % paraformaldehyde for 15 min. Finally, the cells were subjected to observation by a confocal laser scanning microscope.

Synthesis of 3

A three neck flask was charged with **4** (181.2 mg, 0.6 mmol), **5** (111.0 mg, 0.5 mmol), K_2CO_3 (400.5 mg, 2.89 mmol), toluene (50 mL) and H_2O (12.5 mL), the resulting solution was degassed via three freeze-pump-thaw cycles. $Pd(PPh_3)_4$ (107.2 mg, 0.0926 mmol) was then added under an argon atmosphere. The mixture was refluxed for about 1 h (monitored by TLC) resulting in a turbid solution. After the solvent was removed under vacuum, CH_2Cl_2 (50 mL) was added and washed with H_2O. The organic layer was dried with anhydrous Na_2SO_4 and filtered. Then removal of CH_2Cl_2 under vacuum, the residue was purified by column chromatography on SiO_2 with CH_2Cl_2 as eluent to give light yellow solid (110.2 mg, 61 %). ^{1}H NMR (400 MHz, $CDCl_3$) δ 8.70 (s, 2H), 8.57 (s, 1H), 8.47 (d, *J* = 15.7 Hz, 2H), 8.17 (d, *J* = 8.8 Hz, 1H), 8.05 (s, 2H), 7.83 (d, *J* = 8.7 Hz, 1H), 7.54 (s, 2H), 4.56 (dd, *J* = 14.0, 6.9 Hz, 4H), 1.51 (t, *J* = 7.0 Hz, 6H). ^{13}C NMR (101 MHz, $CDCl_3$) δ 163.9, 149.8, 148.2, 131.8, 131.5, 131.2, 130.3, 130.1, 128.7, 127.3, 127.2, 126.6, 125.3, 125.2, 125.0, 124.5, 122.4, 98.9, 61.5, 13.2. HR-MS (ESI): m/z calcd for $C_{25}H_{21}NO_4$: 400.1549 $[M+H]^+$, found: 400.1547 (Fig. S1-S3).

Synthesis of 1

Sodium hydroxide (30.3 mg, 0.75mmol) was dissolved in water (10 mL) and 10 mL THF solution of 3 (50.4 mg, 0.125 mmol) was added. The resulting suspension was stirred at 100 °C overnight and cooled to room temperature. After removal of

View Article Online
DOI: 10.1039/C9SC00026G

THF under vacuum, the pH was adjusted to 1 using 37% aqueous hydrogen chloride solution. The resulting precipitate was filtered off, washed with water (3 x 30 mL) and dried under vacuum. The product was obtained as a yellow solid (37.4 mg, 74 %). ^{1}H NMR (400 MHz, DMSO) δ 8.81 (s, 2H), 8.68 (s, 3H), 8.29 (d, *J* = 8.9 Hz, 1H), 8.14 (d, *J* = 6.5 Hz, 2H), 8.05 (d, *J* = 9.6 Hz, 1H), 7.64 – 7.51 (m, 2H). ^{13}C NMR (101 MHz, DMSO) δ 166.0, 150.2, 149.8, 145.9, 132.9, 132.5, 132.1, 131.5, 131.4, 130.0, 128.7, 128.6, 128.2, 128.0, 126.8, 126.5, 124.9, 124.2. HR-MS(ESI): m/z calcd. for $C_{21}H_{13}NO_4$: 344.0924 $[M+H]^+$, found: 344.0918 (Fig. S4-S6) .

Determination of association constant (*K*)

In the UV-vis titration experiments, the association constant (K_a) for a stoichiometric 1:2 complex (γ-CD·**1**$_2$) of γ-CD with **1** was calculated by using the non-linear least-squares fit of the titration data according to the following formula with the Origin program.[17]

$$\Delta A_{obs} = \frac{\varepsilon_{\Delta HG}[G]_0 K_1[H] + 2\varepsilon_{\Delta HG_2}[G]_0 K_1 K_2[H]^2}{1 + K_1[H] + K_1 K_2[H]^2}$$

where ΔA_{obs} is the UV-vis absorption change of **1** upon addition of γ-CD. K_1 and K_2 are the first-order bonding constant and the second-order bonding constant, respectively. $\varepsilon_{\Delta HG}$ is the molar absorption coefficient changes between the γ-CD·**1** inclusion complex and **1**. $\varepsilon_{\Delta HG2}$ is the molar absorption coefficient changes between the γ-CD·**1**$_2$ inclusion complex and **1**. $[G_0]$ is the initial concentration of guest molecule.

Preparation of Eu complex

Europium(III) nitrate hexahydrate ($Eu(NO_3)_3 \cdot 6H_2O$) was purchased from Energy Chemical. A certain amount of $Eu(NO_3)_3$ was dissolved in deionized water, then added to the aqueous solution of **1** or γ-CD·**1**$_2$ to prepare the Eu complex in situ. Preparation of Eu^{3+}⊂γ-CD·**1**$_2$, i.e. Eu complex of γ-CD·**1**$_2$, as an example: A solution of $Eu(NO_3)_3$ (2 mM) was prepared in deionized water, then 45 μL of the $Eu(NO_3)_3$ solution was added to the aqueous solution of γ-CD·**1**$_2$ (0.1 mM, 3 mL) to obtain the Eu^{3+}⊂γ-CD·**1**$_2$ solution (0.1 mM).

Results and discussion

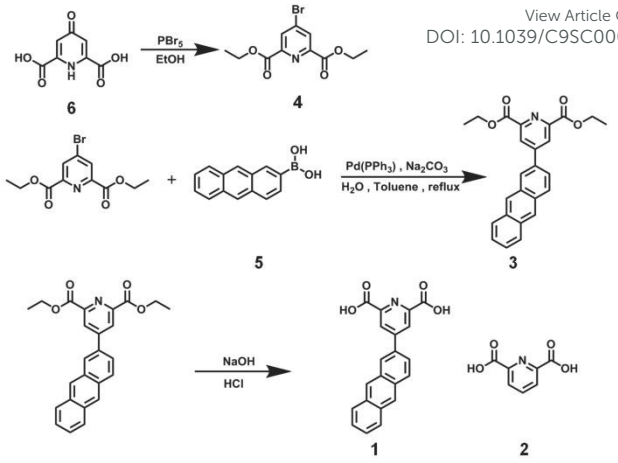

Scheme 1. Synthetic scheme of **1** and the structure of **2**

1 was prepared in 74 % yield via a Suzuki reaction of diethyl 4-bromopyridine-2,6-dicarboxylate with 2-anthraceneboronic acid under a alkaline condition, followed by a subsequent hydrolysis reaction(Scheme 1). It was reported that the γ-CD cavity could accommodate two 2-anthryl groups, and the 1 : 2 inclusion complex had four possible configurations including *syn* or *anti* head-to-tail (HT) and head-to-head (HH) isomers in aqueous solution.[18] Herein, the similar phenomenon was observed in aqueous solution. Fig S7a showed the UV-vis absorption and fluorescence emission of **1**. The UV-vis spectra (Fig. 2a, S7b) showed that, with the stepwise addition of γ-CD, the ^1B_b band of **1** at 260-280 nm gradually decreased, indicating the conformational change from the J-aggregate of self-assembled **1** to the H-aggregate of diploid **1** due to the inclusion of γ-CD cavity.[18] In addition, the ^1L_a band of **1** at 410 nm showed a little bathochromic shift, and its intensity decreased. Moreover, two apparent isosbestic points at 319 nm and 400 nm were also observed. These phenomena jointly indicated the conversion of free **1** to the γ-CD·**1**$_2$ inclusion complex.[19] Accordingly, the association constants (K_a) between **1** and γ-CD were calculated to be K_{a1} = 4.38 × 10^2 M^{-1} and K_{a2} = 5.58 × 10^4 M^{-1} at 25°C by analyzing the sequential changes in UV-vis spectra (ΔA) of **1** at varying concentrations of γ-CD using a nonlinear least-squares curve-fitting method according to literature reports (Fig. 2a and Fig. S7c).[17] The Job's plot gave an inflection point at a molar ratio of 0.667, corresponding to a 1:2 host-guest inclusion stoichiometry (Fig. S8), which was consistent with the previously reported result.[19] To further prove the inclusion, ^{1}H NMR spectra (Fig. S9a, b) showed that the anthracene protons shifted upfield 0.375-0.4 ppm upon the complexation with γ-CD. In the circular dichroism spectra (Fig. S10), the γ-CD·**1**$_2$ inclusion complex (green line) showed a positive Cotton effect peak at 350-400 nm and a negative Cotton effect peak at 400-450 nm, indicating the formation of a pseudo[3]rotaxanes.[19c] In the fluorescence spectra (Fig. 2b), the fluorescence intensity of **1** appreciably decreased with the gradual addition of γ-CD, due to the π-π stacked of **1** in the hydrophobic γ-CD cavity. Considering the structure of **1** that has a bulky negatively charged substituent at 2-

position, we deduced that two units of **1** tended to adopt a *syn* or *anti* head-to-tail (HT) conformation upon inclusion by γ-CD.

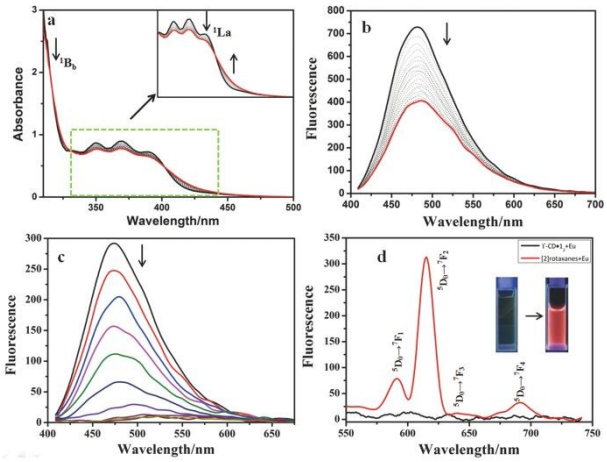

Fig. 2 (a) Absorption spectra and (b) emission spectra of **1** (0.2 mM) with (red) and without (black) γ-CD (0-0.3 mM) at pH 9.0 in water(25 °C). (c) Emission spectra of γ-CD·$\mathbf{1}_2$ (0.2 mM) upon addition of Eu^{3+} (from 0 to 3eq) at pH 9.0 in water (25 °C, λ_{ex} =365 nm) (d) Emission spectra of Eu^{3+}⊂γ-CD·$\mathbf{1}_2$ system (black) and Eu^{3+}⊂[2]rotaxanes (red) at 25 °C. Inset: photo image of fluorescence in pH 9.0 aqueous solution under UV light. (λ_{ex}=254 nm, 254 nm used as an excitation source).

It was well reported that pyridine-2,6-dicarboxylic acid (DPA) could strongly coordinate lanthanide ions with a ratio of 3:1.[20] Similarly, the fluorescence spectral experiments showed the 1:3 coordination stoichiometry between Eu^{3+} and **1**, which was consistent with our previous observation (Fig. S11).[13c] Possessing two terminal DPA units, γ-CD·$\mathbf{1}_2$ complex also showed the similar coordination behaviors with lanthanide ions (Fig. 2c). With the gradual addition of Eu^{3+} to γ-CD·$\mathbf{1}_2$ complex, no characteristic fluorescence of Eu^{3+} could be observed, but the fluorescence at 480 nm, assigned to the intrinsic blue fluorescence of ligand, gradually quenched (Fig. 2c, 2d black line), similar to the previously report.[13c] A possible reason may be that a large aromatic conjugate system in the antenna molecule led to a mismatch between the lowest triplet state of ligand and the first excited state of lanthanide. It is well-documented that anthracenes are photoresponsive and be apt to photodimerization under UV irradiation.[21] However, after irradiating the aqueous solution of Eu^{3+}⊂γ-CD·$\mathbf{1}_2$ under N_2 for 16 min at 365 nm with an intensity of 50 W, the resultant solution presented four characteristic emissions (Fig. 2d, red line) of Eu^{3+} at 590 nm ($^5D_0 \rightarrow {}^7F_1$), 615 nm ($^5D_0 \rightarrow {}^7F_2$), 645 nm ($^5D_0 \rightarrow {}^7F_3$) and 680 nm ($^5D_0 \rightarrow {}^7F_4$),[13] which was quite similar to that of Eu^{3+}⊂$\mathbf{2}_3$ (Fig. S12). This means that an energy transfer (ET) process occurred from pyridine-2,6-dicarboxylic acid (DPA) to Eu^{3+}.[13c] In the ^1H NMR spectra, the proton signals at 7.0-7.6 ppm assigned to the anthanence group in **1** displayed an upfield shift (Fig. S9), indicating that two accommodated groups may undergo a dimerization after the UV light irradiation.[19c] Moreover, the ROESY spectrum (Fig. S13) also showed the clear NOE(Nuclear Overhauser Effect) correlations between the dimeric anthanence groups and the inner protons of γ-CD. In addition, the circular dichroism spectrum (Fig. S10) of γ-CD·$\mathbf{1}_2$ after UV irradiation was obviously different from that before UV irradiation. The ESI-MS spectrum of Eu^{3+}⊂γ-CD·$\mathbf{1}_2$ after irradiation under 365 nm in water showed a clear signal at m/z 1981.1 assigned to the [2]rotaxane, while the ESI-MS spectrum of a highly concentrated THF solution of **1** after irradiation under 365 nm showed a signal at m/z 689.1 assigned to the dimer of **1** (Fig. S14, S15). No ESI-MS signal of photooxidized product was observed for the case of either **1** or γ-CD·$\mathbf{1}_2$. These phenomena jointly demonstrated that two discrete units of **1** in a γ-CD cavity converted into a dimer, i.e. γ-CD·$\mathbf{1}_2$ complex converted to a [2]rotaxane, after UV light irradiation, and the photodimerized product was the principal product. Therefore, a possible emission mechanism could be deduced as follow: the photo-dimerization of two accommodated anthracene groups in the γ-CD cavity destroyed the large conjugated structure of γ-CD·$\mathbf{1}_2$, allowing the match of the lowest triplet state of ligand to the first excited state of lanthanide ion. As a result, the characteristic fluorescence of Eu^{3+} was presented.[13c]

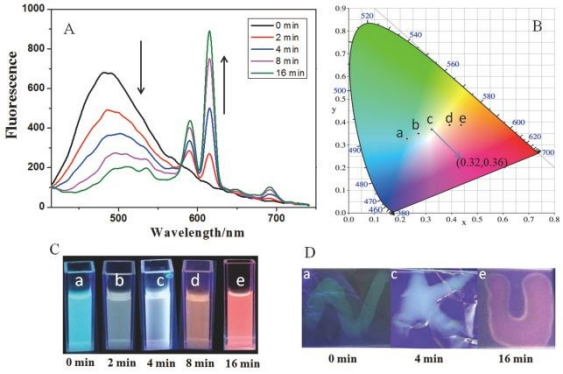

Fig. 3 (A) Emission spectra (λ_{ex} = 290 nm) of Eu^{3+}⊂γ-CD·$\mathbf{1}_2$ ([$\mathbf{1}_2$]=0.1 mM, [Eu^{3+}]=0.03 mM) at initial state (a) and after photoirradiation for (b) 2 min, (c) 4 min, (d) 8 min, and (e) 16 min in pH=9.0 aqueous solution at 25 °C; (B) CIE 1931 chromaticity diagram. The black dots signify the luminescent color coordinates for the corresponding states a (0.22, 0.32), b (0.27, 0.34), c (0.32, 0.36), d (0.39, 0.38), and e (0.43, 0.38). (C) The images of the corresponding states under UV irradiation (λ_{ex} = 365 nm), and (D) the features of fluorescent inks based on the Eu^{3+}⊂γ-CD·$\mathbf{1}_2$-doped PVA (The molar ratio is 1:500) film under UV irradiation (λ_{ex} = 365 nm).

Significantly, Eu^{3+}⊂γ-CD·$\mathbf{1}_2$ showed the different emission color with the changes of light irradiation times. Without the light irradiation, Eu^{3+}⊂γ-CD·$\mathbf{1}_2$ only emitted the intrinsic blue fluorescence of ligand (Fig. 3A) at 490 nm. After irradiating the solution of Eu^{3+}⊂γ-CD·$\mathbf{1}_2$ under N_2 at 365 nm for 16 min, the fluorescence emission of Eu^{3+} gradually enhanced, and the emission color changed in an order of cyan (0 min) → pale yellow (2 min) → white (4 min) → orange (8 min) → red (16 min). Moreover, an obvious white-light point with the CIE coordinate (0.32, 0.36) was observed in the CIE 1931 chromaticity diagram (Fig. 3B). A possible reason may be that, with the continuous irradiation of UV light irradiation, Eu^{3+}⊂γ-CD·$\mathbf{1}_2$, which emitted the cyan fluorescence, gradually converted to Eu^{3+}⊂[2]rotaxane that emitted the red

fluorescence. Therefore, at different time points, the Eu^{3+}⊂γ-CD·**1**$_2$ system existed as the mixtures of blue-light species Eu^{3+}⊂γ-CD·**1**$_2$ and red-light species Eu^{3+}⊂[2]rotaxane with different ratios, leading to the multi-color emission including white light. In addition, fluorescence lifetime experiments showed that the decay curve in pH 9.0 water followed a double exponential decay with a fluorescence lifetimes at τ_1 = 1.10 ns and τ_2 = 5.97 ns at initial state, and no fluorescence lifetimes of lanthanide ions were observed. But the Eu^{3+}⊂γ-CD·**1**$_2$ showed the fluorescence lifetimes of lanthanide ions at τ_1 = 251.88 μs and τ_2 = 993.46 μs after photoirradiation for 16 min (Fig. S16). The quantum yields were 3.12 % at initial state, 2.67 % at 4 min and 15.74 % at 16 min. In the emission spectra of Eu^{3+}⊂γ-CD·**1**$_2$ without photoirradiation, i.e. the case where the sample is made up and no irradiation, no appreciable emission color changes were observed (Fig. S17a), indicating that the different emission colors are due to the irradiation induced rotaxane formation rather than a simply slow coordination event. In the irradiation study of Eu^{3+}⊂**1**$_3$ complex (i.e. no CD present), very slight color changes were observed after irradiating Eu^{3+}⊂**1**$_3$ complex only, indicating that the CD is required for the different emission colors because CD can not only increase the solubility of the guest, but also accelerate the dimerization (Fig. S17b). Meanwhile, the changes of absorption spectra and the excitation spectra Eu^{3+}⊂γ-CD·**1**$_2$ with the photoirradiation were shown in Figs S17c-d. Furthermore, the morphology of Eu^{3+}⊂[2]rotaxane was investigated by scanning electron microscopy (SEM) and transmission electron microscopy (TEM) (Fig. S18-S19). In SEM and TEM images, free **1** existed as a number of needle-like nanofibers, and γ-CD·**1**$_2$ showed the morphology as irregular blocks. However, the morphology of Eu^{3+}⊂γ-CD·**1**$_2$ before and after UV light irradiation both existed as thin films. In addition, the zeta potentials of free **1**, γ-CD·**1**$_2$, Eu^{3+}⊂γ-CD·**1**$_2$ were measured to be −29.44 mV, −10.63 mV and −4.45 mV (Fig. S20), respectively, indicating that the coordination of Eu^{3+} decreased the surface electronegativity of **1** or γ-CD·**1**$_2$.

Benefitting from the photo-controlled multicolor emission property, Eu^{3+}⊂γ-CD·**1**$_2$ could be used as a tunable photochromic fluorescence ink. In a typical test, some characters were written with the solution of Eu^{3+}⊂γ-CD·**1**$_2$-doped PVA as ink on an ordinary glass piece, and these characters emitted blue fluorescence under the UV lamp after being dried in air (Fig. 3). When irradiation with the UV light (365 nm) from 0 min to 4 min, the characters emitted white fluorescence, which further turned red after irradiation for 16 min. Interestingly, these multi-color characters could keep stable for at least 72 h without any appreciable fading. Therefore, the tunable photochromic multi-color emission property will enable the application of Eu^{3+}⊂γ-CD·**1**$_2$ assembly as novel anti-counterfeiting materials in which the information and the state could be effectively written and read out by simply alternating the UV irradiation time.

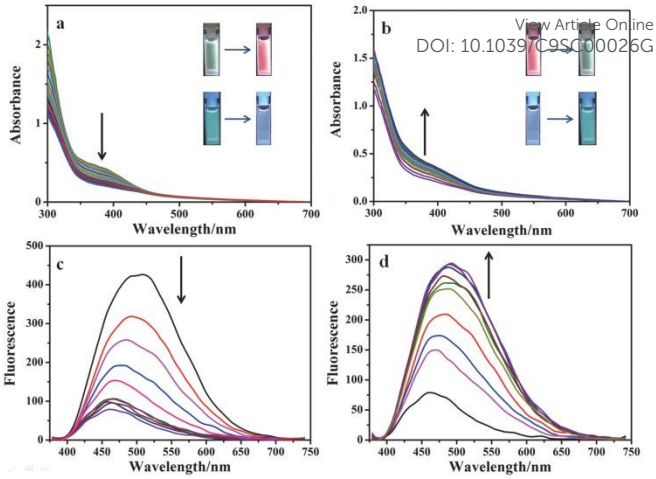

Fig. 4 Absorption spectral changes of Eu^{3+}⊂γ-CD·**1**$_2$ (0.1 mM) upon irradiation (a) at 365 nm and (b) at 254 nm in PBS at 25 °C (pH=7.2, inset: the upper and lower images for the fluorescence images of changing at an excitation source of 254 nm and 365 nm, respectively). Fluorescence spectral changes of Eu^{3+}⊂γ-CD·**1**$_2$ upon photoirradiation (c) at 365 nm and (d) at 254 nm in PBS at 25 °C (λ_{ex} = 365 nm)

In addition to fluorescence ink, the Eu^{3+}⊂γ-CD·**1**$_2$ assembly could also be used as photo-modulated multicolor fluorescence labelling for living cells. Firstly, we study the luminescence behavior under physiological conditions in PBS buffer (PH=7.2). Similarly, the assembly Eu^{3+}⊂γ-CD·**1**$_2$ exhibits red luminescence (at 254 nm) and the white luminescence (at 365 nm) after the light irradiation (Fig. 4a, S21a). Accordingly, UV−vis absorption measurement and fluorescence spectrum were performed to monitor the photodimerization process of anthracene. Irradiation of the Eu^{3+}⊂γ-CD·**1**$_2$ under N_2 with 365 nm light using a portable UV lamp (6 W) decreased the intensity of absorption bands at 373 nm (assigned to π-π* transition bands of anthracene units) and the fluorescence intensity at 494 nm was gradually declined, indicating that the photodimerization disrupted the conjugation of anthracene units (Fig. 4a, 4c).[21,22] Fluorescence lifetime decay curve of Eu^{3+}⊂γ-CD·**1**$_2$ in PBS buffer (pH=7.2) also showed the fairly high fluorescence lifetimes of lanthanide ion up to τ_1 = 543.50 μs and τ_2 = 1204.91 μs after photoirradiation (Fig. S22). Moreover, the reversibility of such luminescence properties is highly desired for wide applications and thus we examined its reversibility. When Eu^{3+}⊂[2]rotaxane was irradiated at 254 nm for 120 s, a reconversion to the parent species Eu^{3+}⊂γ-CD·**1**$_2$ occurred, as confirmed by UV−vis absorption measurement and fluorescence spectrum (Fig. 4b, 4d). Significantly, cycle tests showed that the external-stimuli-responsive transformation is repetitive (Fig. S21b, S23). The solution of free **1** and Eu^{3+}⊂**1**$_3$ quickly precipitated as shown in Fig. S21c. Simultaneously, the fluorescence of Eu^{3+}⊂**1**$_3$ is very weak, and red fluorescence is not observed after irradiated at 365 nm for 3 h or even longer (Fig. S21a). We then treated human lung adenocarcinoma cells (A549 cells) with the Eu^{3+}⊂γ-CD·**1**$_2$ assembly for 24 h. The cytotoxicity of the assembly was evaluated by using a standard MTT assay. As shown in Fig. S24, over 90% cell viability is observed after incubation of A549 cells with the assembly at

concentrations ranging from 1 to 16 μM for 24 h, thus confirming the low cytotoxicity of the assembly. Confocal laser scanning microscopy revealed that the cells initially emitted blue fluorescence in the cytoplasm under the UV irradiation (365 nm) (Fig. 5a), and then gradually emitted white fluorescence after 1 min of irradiation, which remained stable for further irradiation (Fig. 5b). Thus, this assembly could be used to tag cells with white fluorescence. As we know, most of fluorescence dyes only exhibit blue, green, red or yellow fluorescence during cell imaging.[15,23] It is necessary to develop novel staining systems with other fluorescence emission properties when more than four fluorescence signals are needed. The Eu^{3+}⊂γ-CD·$\mathbf{1}_2$ assembly with white light emission provides the fifth kind of fluorescence signal, and hence would have a wide application in multi-color imaging for biological studies.

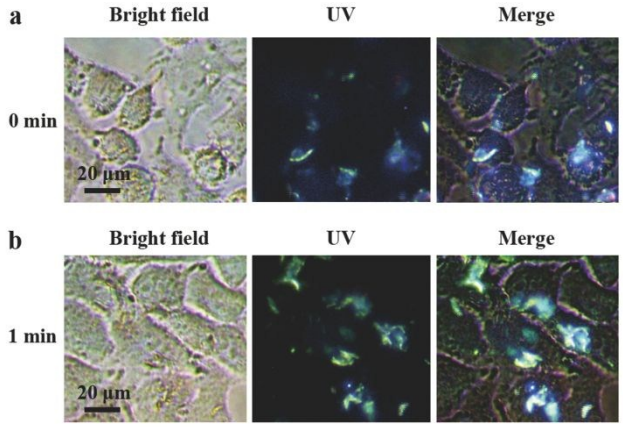

Fig. 5 Confocal fluorescence images of A549 cells with Eu^{3+}⊂γ-CD·$\mathbf{1}_2$ ([Eu^{3+}]= 2 μM, [γ-CD] = 4 μM, [$\mathbf{1}_2$] = 8 μM,) for (a) 0 min, (b) 1 min under UV at 25 °C.

Conclusions

In conclusion, we have successfully constructed a photo-tunable supramolecular assembly from γ-CD, anthracene-modified DPA and lanthanide metal via the time-dependent photo-crosslink reaction. The resultant supramolecular assembly possessed dual emission properties, i.e. a red-light emission of Eu(III) and a blue-light emission of anthyl-modified DPA. Through controllably adjust the light irradiation time, the supramolecular assembly could emit fluorescence with various colors (especially white light) in several environments such as aqueous solution, solid film and especially living cell, which enabled the potential application of this photomodulated multi-color assembly as a tunable photochromic fluorescence ink and cell labelling. We believe this could provide a new strategy for the information processing and biological imaging.

Conflicts of interest

There are no conflicts to declare.

Acknowledgements

We thank NNSFC (21672113, 21432004, 21772099, 21861132001 and 91527301) for financial support.

Notes and references

1 (a) L. Fang, M. A. Olson, D. Benitez, E. Tkatchouk, W. A. Goddard, J. F. Stoddart, *Chem. Soc. Rev.* 2010, **39**, 17-29; (b) H. X. Wang, Z. Meng, J. F. Xiang, Y. X. Xia, Y. H. Sun, S. Z. Hu, H. Chen, J. N. Yao, C. F. Chen, *Chem. Sci.* 2016, **7**, 469-474. (c) Z. J. Zhang, H. Y. Zhang, H. Wang, Y. Liu, *Angew. Chem., Int. Ed.* 2011, **50**, 10834-10838.

2 (a) K. Iwaso, Y. Takashima, A. Harada, *Nat. Chem.* 2016, **8**, 625-632; (b) M. R. Panman, C. N. van Dijk, A. Huerta-Viga, H. J. Sanders, B. H. Bakker, D. A. Leigh, A. M. Brouwer, W. J. Buma, S. Woutersen, *Nat. Commun.* 2017, **8**, 1.

3 (a) A. Ulfkjaer, F. W. Nielsen, H. Al-Kerdi, T. Ruß, Z. K. Nielsen, J. Ulstrup, L. L. Sun, K. Moth-Poulsen, J. D. Zhang, M. Pittelkow, *Nanoscale* 2018, **10**, 9133-9140; (b) M. W. Ambrogio, C. R. Thomas, Y. L. Zhao, J. I. Zink, J. F. Stoddart, *Acc. Chem. Res.* 2011, **44**, 903-913.

4 (a) S. Erbas-Cakmak, S. D. P. Fielden, U. Karaca, D. A. Leigh, C. T. McTernan, D. J. Tetlow, M. R. Wilson, *Science* 2017, **358**, 340-343; (b) S. Kassem, A. T. L. Lee, D. A. Leigh, V. Marcos, L. I. Palmer, S. Pisano, *Nature* 2017, **549**, 374-378; (c) M. Mohankumar, M. Holler, E. Meichsner, J. F. Nierengarten, F. Niess, J. P. Sauvage, B. Delavaux-Nicot, E. Leoni, F. Monti, J. M. Malicka, M. Cocchi, E. Bandini, N. Armaroli, *J. Am. Chem. Soc.* 2018, **140**, 2336-2347.

5 (a) X. Ma, H. Tian, *Chem. Soc. Rev.* 2010, **39**, 70-80; (b) X. Hou, C. Ke, C. J. Bruns, P. R. McGonigal, R. B. Pettman, J. F. Stoddart, *Nat. Commun.* 2015, **6**, 6884; (c) M. Inouye, K. Hayashi, Y. Yonenaga, T. Itou, K. Fujimoto, T. Uchida, M. Iwamura, K. Nozaki, *Angew. Chem., Int. Ed.* 2014, **53**, 14392-14396; (d) L. D. Movsisyan, M. Franz, F. Hampel, A. L. Thompson, R. R. Tykwinski, H. L. Anderson, *J. Am. Chem. Soc.* 2016, **138**, 1366-1376.

6 (a) G. M. Farinola, R. Ragni, *Chem. Soc. Rev.* 2011, **40**, 3467-3482; (b) O. Kotova, S. Comby, C. Lincheneau, T. Gunnlaugsson, *Chem. Sci.* 2017, **8**, 3419-3426; (c) S. Reineke, F. Lindner, G. Schwartz, N. Seidler, K. Walzer, B. Lussem, K. Leo, *Nature* 2009, **459**, 234-238.

7 (a) B. W. D' Andrade, S. R. Forrest, *Adv. Mater.* 2004, **16**, 1585-1595; (b) K. T. Kamtekar, A. P. Monkman, M. R. Bryce, *Adv. Mater.* 2010, **22**, 572-582; (c) L. L. Zhu, C. Y. Ang, X. Li, K. T. Nguyen, S. Y. Tan, H. Agren, Y. L. Zhao, *Adv. Mater.* 2012, **24**, 4020-4024.

8 (a) M. M. Shang, C. X. Li, J. Lin, *Chem. Soc. Rev.* 2014, **43**, 1372-1386; (b) N. Willis-Fox, M. Kraft, J. Arlt, U. Scherf, R. C. Evans, *Adv. Funct. Mater.* 2016, **26**, 532-542. (c) X. Feng, C. X. Qi, H. T. Feng, Z. Zhao, H. H. Y. Sung, I. D. Williams, R. T. K. Kwok, J. W. Y. Lam, A. J. Qin, B. Z. Tang, *Chem. Sci.* 2018, **9**, 5679–5687.

9 (a) R. Abbel, C. Grenier, M. J. Pouderoijen, J. W. Stouwdam, P. E. L. G. Leclere, R. P. Sijbesma, E. W. Meijer, A. P. H. J. Schenning, *J. Am. Chem. Soc.* 2009, **131**, 833-843; (b) Z. Y. Zhang, B. Xu, J. H. Su, L. P. Shen, Y. S. Xie, H. Tian, *Angew. Chem., Int. Ed.* 2011, **123**, 11858-11861; (c) Q. Zhao, Y. Chen, S. H. Li, Y. Liu, *Chem. Commun.* 2018, **54**, 200-203.

10 Q. W. Zhang, D. F. Li, X. Li, P. B. White, J. Mecinovic, X. Ma, H. Agren, R. J. M. Nolte, H. Tian, *J. Am. Chem. Soc.* 2016, **138**, 13541-13550.

11 X. L. Ni, S. Y. Chen, Y. P. Yang, Z. Tao, *J. Am. Chem. Soc.* 2016, **138**, 6177-6183.

12 S. H. Li, X. F. Xu, Y. Zhou, Q. Zhao, Y. Liu, *Org. Lett.* 2017, **19**, 6650-6653.

13 (a) H. B. Cheng, H. Y. Zhang, Y. Liu, *J. Am. Chem. Soc.* 2013, **135**, 10190-10193; (b) M. Isaac, S. A. Denisov, A. Roux, D. Imbert, G. Jonusauskas, N. D. McClenaghan, O. Seneque, *Angew. Chem.* 2015, **127**, 11615-11618; (c) Y. Zhou, H. Y. Zhang, Z. Y. Zhang, Y. Liu, *J. Am. Chem. Soc.* 2017, **139**, 7168-

View Article Online
DOI: 10.1039/C9SC00026G

7171; (d) B. McMahon, T. Gunnlaugsson, *J. Am. Chem. Soc.* 2012, **134**, 10725-10728; (e)O. Kotova, R. Daly, C. M. G. dos Santos, M. Boese, P. E. Kruger, J. J. Boland, T. Gunnlaugsson, *Angew. Chem.* 2012, **51**, 7208-7212.
14 H. Wu, Y. Chen, Y. Liu, *Adv. Mater.* 2017, **29**, 1605271.
15 X-M. Chen, Y. Chen, Q. L. Yu, B-H. Gu, Y. Liu, *Angew. Chem., Int. Ed.* 2018, **57**, 12519-12523.
16 K. E. Pryor, G. W. Shipps Jr., D. A. Skyler, J. Rebek Jr., *Tetrahedron* 1998, **54**, 4107-4124.
17 (a) P. Thordarson, *Chem. Soc. Rev.* 2011, **40**, 1305-1323; (b) H. Bakirci, X. Zhang, W. M. Nau, *J. Org. Chem.* 2005, **70**, 39-46.
18 (a) A. Wakai, H. Fukasawa, C. Yang, T. Mori, Y. Inoue, *J. Am. Chem. Soc.* 2012, **134**, 4990-4997; (b) Q. Wang, C. Yang, C. F. Ke, G. Fukuhara, T. Mori, Y. Liu, Y. Inoue, *Chem. Commun.* 2011, **47**, 6849-6851; (c) C. Yang, Y. Inoue, *Chem. Soc. Rev.* 2014, **43**, 4123-4143.
19 (a) A. Nakamura, Y. Inoue, *J. Am. Chem. Soc.* 2003, **125**, 966-972; (b) X. Q. Wei, W. H. Wu, R. Matsushita, Z. Q. Yan, D. Y. Zhou, J. J. Chruma, M. Nishijima, G. Fukuhara, T. Mori, Y. Inoue, C. Yang, *J. Am. Chem. Soc.* 2018, **140**, 3959-3974; (c) C. Yang, T. Mori, Y. Origane, Y. H. Ko, N. Selvapalam, K. Kim, Y. Inoue, *J. Am. Chem. Soc.* 2008, **130**, 8574-8575;
20 (a) Z. Q. Li, G. N. Wang, Y. G. Wang, H. R. Li, *Angew. Chem., Int. Ed.* 2018, **57**, 2194-2198; (b) Y. Liu, G. S. Chen, Y. Chen, N. Zhang, J. Chen, Y. L. Zhao, *Nano Lett.* 2006, **6**, 2196-2200.
21 (a) Z. A. Huang, C. Chen, X. D. Yang, X. B. Fan, W. Zhou, C. H. Tung, L. Z. Wu, H. Cong, *J. Am. Chem. Soc.* 2016, **138**, 11144-11147; (b) D. J. Murray, D. D. Patterson, P. Payamyar, R. Bhola, W. T. Song, M. Lackinger, A. D. Schluter, B. T. King, *J. Am. Chem. Soc.* 2015, **137**, 3450-3453; (c) T. Yamamoto, S. Yagyu, Y. Tezuka, *J. Am. Chem. Soc.* 2016, **138**, 3904-3911; (d) P. F. Wei, X. Z. Yan, F. H. Huang, *Chem. Commun.* 2014, **50**, 14105-14108; (e) G. Collet, T. Lathion, C. Besnard, C. Piguet, S. Petoud, *J. Am. Chem. Soc.* 2018, **140**, 10820-10828.
22 (a) H. Bouas-Laurent, A. Castellan, J-P. Desvergnea, R. Lapouyade, *Chem. Soc. Rev.* 2000, **29**, 43-55; (b) N. Huang, X. Ding, J. Kim, H. Ihee, D. Jiang, *Angew. Chem., Int. Ed.* 2015, **54**, 8704-8707.
23 (a) K. Jiang, S. Sun, L. Zhang, Y. Lu, A. Wu, C. Cai, H. Lin, *Angew. Chem., Int. Ed.* 2015, **54**, 5360-5363; (b) Q. L. Yu, Y-M. Zhang, Y-H. Liu, X. Xu, Y. Liu, *Sci. Adv.* 2018, **4**, eaat2297; (c) G. C. Yu, Z. Yang, X. Fu, B. C. Yung, J. Yang, Z. W. Mao, L. Shao, B. Hua, Y. Liu, F. Zhang, Q. Fan, S. Wang, O. Jacobson, A. Jin, C. Y. Gao, X. Tang, F. H. Huang, X. Y. Chen, *Nat. Commun.* 2018, **9**, 9.

View Article Online
DOI: 10.1039/C9SC00026G

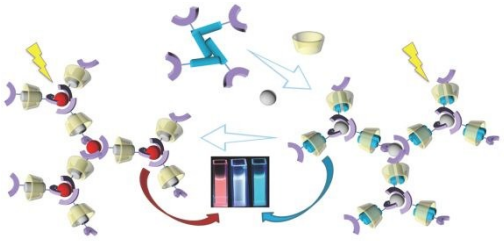

Photo-responsive Cyclodextrin/Anthracene/Eu^{3+} Supramolecular Assembly for a Tunable Photochromic Multicolor Cell Label and Fluorescent Ink

Weilei Zhou,[a] Yong Chen,[a] Qilin Yu,[a,c] Peiyu Li,[a] Xuman Chen[a] and Yu Liu*[a,b]

A photoresponsive supramolecular assembly was constructed and presented multi-color fluorescence emissions in several environments including solution, PVA and living cell.